JOURNAL OF GEOPHYSICAL RESEARCH, VOL. 113, D15305, doi:10.1029/2007JD009428, 2008

Trans-Pacific transport of mercury

Sarah A. Strode,[1] Lyatt Jaeglé,[1] Daniel A. Jaffe,[2] Philip C. Swartzendruber,[1,2] Noelle E. Selin,[3] Christopher Holmes,[3] and Robert M. Yantosca[3]

Received 27 September 2007; revised 24 December 2007; accepted 25 March 2008; published 7 August 2008.

[1] We examine the trans-Pacific transport of mercury with a global chemical transport model. Using existing anthropogenic inventories, the model underestimates the observed Hg/CO ratio in Asian long-range transport events observed at ground-based sites in Okinawa, Japan and Mount Bachelor, Oregon, by 18–26%. This is in contrast with previous studies that inferred a factor of two underestimate in Asian anthropogenic emissions. We find that mercury from land emissions and re-emissions, which are largely colocated with anthropogenic emissions, account for a significant fraction of the observed Hg/CO ratio. Increasing Asian anthropogenic Hg^0 emissions by 50% while holding land emissions constant, or further increasing anthropogenic emissions while decreasing land emissions, corrects the remaining model bias in the Hg/CO ratio. We thus find that a total Asian source of 1260–1470 Mg/a Hg^0 is consistent with observations. Hg^0 emissions from Asia are transported northeastward across the Pacific, similar to CO. Asian anthropogenic emissions of mercury contribute 18% to springtime Hg^0 concentrations at Mount Bachelor. Asian RGM is not directly transported to North America in the lower troposphere but contributes to a well-mixed pool at high altitude. Asian and North American sources each contribute approximately 25% to deposition to the United States, with Asian anthropogenic sources contributing 14% and North American anthropogenic sources contributing 16%.

Citation: Strode, S. A., L. Jaeglé, D. A. Jaffe, P. C. Swartzendruber, N. E. Selin, C. Holmes, and R. M. Yantosca (2008), Trans-Pacific transport of mercury, *J. Geophys. Res.*, *113*, D15305, doi:10.1029/2007JD009428.

1. Introduction

[2] Anthropogenic emissions have caused a factor of 3 increase in the atmospheric mercury burden since preindustrial times [*Mason and Sheu*, 2002], posing a threat to human health and wildlife. Asian emissions increased rapidly in the early 1990s, and in 2000 accounted for 54% of global anthropogenic emissions [*Pacyna et al.*, 2006]. European and North American emissions decreased over the same time period.

[3] With an atmospheric lifetime of several months, elemental mercury (Hg^0) undergoes global atmospheric transport. Global modeling studies indicate that 21–24% of mercury deposition to North America is of Asian origin, compared to 30–33% of North American origin [*Seigneur et al.*, 2004; *Travnikov*, 2005].

[4] Several observational studies have detected long-range transport of mercury from Asia. Aircraft measurements during the ACE-Asia campaign found mercury to be well correlated with other pollutants in plumes over the western Pacific Ocean [*Friedli et al.*, 2004]. At a ground-based site in Okinawa, Japan, *Jaffe et al.* [2005] measured elevated Hg^0 and CO concentrations during episodes of Asian outflow. During the INTEX-B campaign, *Talbot et al.* [2007] observed mercury in Asian plumes on flights over the Pacific. In North America, observations from Mount Bachelor Observatory, Oregon (MBO) identified episodes of Asian long-range transport with high Hg^0 concentrations [*Jaffe et al.*, 2005; *Weiss-Penzias et al.*, 2006]. The Hg^0/CO enhancement ratio during Asian transport events, which represents the relative increase of the two species over their respective background levels, is expected to reflect the relative emissions of Hg^0 and CO. However, the Okinawa Hg^0/CO enhancement ratio of 0.0056 ng/m^3/ppbv observed during Asian long-range transport events is almost twice the emission ratio from the current anthropogenic mercury and CO inventories [*Jaffe et al.*, 2005]. *Friedli et al.* [2004] and *Weiss-Penzias et al.* [2007] reported similarly enhanced ratios for long-range transport events observed during ACE-Asia and at MBO, respectively. *Jaffe et al.* [2005] proposed three possible explanations for this discrepancy: an underestimate of Asian anthropogenic Hg^0 emissions, a contribution from Asian land emissions, or production of Hg^0 from reactive gaseous mercury (RGM) emissions during transport.

[5] In this paper, we use the GEOS-Chem global chemical transport model to interpret mercury and CO observations at Okinawa, Japan and Mount Bachelor, Oregon. We

[1]Department of Atmospheric Sciences, University of Washington, Seattle, Washington, USA.
[2]Interdisciplinary Arts and Sciences Department, University of Washington, Bothell, Washington, USA.
[3]School of Engineering and Applied Sciences and Department of Earth and Planetary Sciences, Harvard University, Cambridge, Massachusetts, USA.

0148-0227/08/2007JD009428$09.00

use the model to improve constraints on the magnitude of Asian mercury emissions and their contribution to deposition over North America.

2. Observations and Model

[6] The Hedo Station, Okinawa (HSO) is located at 26.8°N, 128.2°E, 60 m above sea level. It is remote from any major cities and in the pathway of East Asian outflow. *Jaffe et al.* [2005] conducted a campaign at Okinawa from 23 March to 2 May 2004, measuring concentrations of mercury species (Hg^0, RGM, and particulate mercury) and CO.

[7] MBO is a mountain top site located at 44.0°N, 121.7°W, 2.8 km above sea level. It receives both free-tropospheric and boundary layer air masses and experiences a diurnal cycle of upslope and downslope flow [*Weiss-Penzias et al.*, 2006]. *Weiss-Penzias et al.* [2006, 2007] describe measurements of total airborne mercury (TAM = Hg^0 + RGM + particulate mercury), CO, and other species at MBO from 28 March 2004 until 30 September 2005. From 30 April to 31 August 2005, *Swartzendruber et al.* [2006] measured speciated mercury (Hg^0, RGM, and particulate mercury) at MBO.

[8] We analyze these observations with the GEOS-Chem global tropospheric chemistry model [*Bey et al.*, 2001] version 7-04-05 (http://www.as.harvard.edu/chemistry/trop/geos/). The model is driven by assimilated meteorology from the NASA Global Modeling and Assimilation Office (GMAO). After a spin-up period to reach steady state, we run the model for 2004 using the GEOS-4 meteorological fields. The model has 2° latitude by 2.5° longitude horizontal resolution and 30 hybrid pressure-sigma layers. For the grid boxes corresponding to Okinawa and MBO, we extract hourly output from the model.

[9] We perform a CO simulation [*Duncan et al.*, 2007], which includes emissions from fossil fuel, biofuel, and climatological biomass burning, as well as a photochemical source from oxidation of methane and biogenic volatile organic compounds (BVOCs). The CO simulation has been evaluated extensively in other studies [e.g., *Heald et al.*, 2003; *Palmer et al.*, 2003; *Liang et al.*, 2004; *Duncan et al.*, 2007].

[10] We also perform a mercury simulation, with tracers for Hg^0, divalent mercury (Hg^{II}), and particulate mercury (Hg^P) [*Selin et al.*, 2007]. We treat the Hg^{II} tracer as comparable to RGM measurements. In the atmosphere, Hg^0 is oxidized to Hg^{II} by ozone and OH, and in cloudy regions Hg^{II} can be reduced back to Hg^0. Hg^{II} is lost through wet and dry deposition. In the rest of the paper we will refer to RGM as Hg^{II}. The model includes emission, transport, and deposition of Hg^P, but does not currently include Hg^P chemistry. The atmospheric mercury model is fully coupled to a slab model of the ocean mixed layer [*Strode et al.*, 2007]. Mercury entering the ocean mixed layer through deposition or oceanic mixing can be converted in the ocean to elemental mercury and then emitted to the atmosphere through gas-exchange, or it can be lost to the deep ocean through mixing and sinking on particles.

[11] The mercury simulation includes emissions from anthropogenic sources [*Pacyna et al.*, 2006; *Wilson et al.*, 2006], biomass burning, and natural emissions plus re-emissions from land and ocean. Globally, the model includes 2200 Mg a^{-1} total mercury from anthropogenic sources, 2000 Mg a^{-1} from land emissions and re-emissions, 520 Mg a^{-1} from biomass burning, and 2970 Mg a^{-1} ocean emissions. Mercury from biomass burning is scaled to climatological biomass burning emissions of CO [*Duncan et al.*, 2003], using a Hg^0/CO emission ratio of 1.5×10^{-7} mol/mol [*Slemr et al.*, 2006b]. Land emissions are divided into a natural (geogenic) component of 500 Mg a^{-1}, distributed in regions with geologic deposits, and a re-emission component of 1500 Mg a^{-1}, distributed according to the pattern of deposition. Ocean emissions are a function of deposition, radiation, biological productivity, temperature, and wind speed. Land, biomass burning, and ocean emissions are all as Hg^0.

[12] Figure 1 shows the distribution of anthropogenic, land, and biomass burning emissions over Asia (defined here as 9°S–60°N, 65°–146°W). For this region, anthropogenic emissions are 610 Mg a^{-1} of Hg^0, 380 Mg a^{-1} of Hg^{II}, and 100 Mg a^{-1} of Hg^P. Geogenic emissions of 100 Mg a^{-1} Hg^0 are located primarily in southeast China. Land re-emissions of 310 Mg a^{-1} Hg^0 are distributed throughout the region, with large emissions from southeast China and India. Large anthropogenic emissions and high deposition rates drive the elevated re-emissions in China. India has lower anthropogenic emissions than China, but its land re-emissions are elevated because high precipitation combined with the elevated rate of Hg^{II} formation in the tropics causes high deposition to this area. Biomass burning accounts for 150 Mg a^{-1} Hg^0, with large emissions from Southeast Asia and India peaking in March and April and emissions from Siberian boreal forest fires peaking in July and August. This region also includes ocean emissions of 360 Mg a^{-1} Hg^0.

[13] Both CO and mercury tracers are tagged in the model according to their emission region and source. We consider four regions: Asia, North America, Europe, and the rest of the world. For mercury, we also tag emissions from biomass burning, land, and ocean sources. The regional land tracers include both geogenic land emissions and land re-emissions. Mercury emitted as Hg^0 that later oxidizes to Hg^{II} retains the tag of its original emission region. For example, the Asian Hg^{II} tracer contains both Hg^{II} directly emitted from Asia and Hg^{II} formed by oxidation of Asian Hg^0. Ocean emissions are tagged as primary ocean only if the mercury entered the mixed layer from the deep ocean; mercury of anthropogenic or land origin that is deposited to the ocean and then re-emitted retains its original tag. Our Asian anthropogenic mercury tracer thus includes both direct emissions from Asia and also ocean re-emission of previously deposited Asian anthropogenic mercury. We infer the contribution to each tracer from ocean re-emission by differencing our standard simulation with a model simulation with the net sea-air flux set to zero. For CO, we tag emissions from anthropogenic (fossil fuel plus biofuel) sources, biomass burning, and the photochemical oxidation of methane and BVOCs.

3. Results

3.1. Hg^0 and CO at Okinawa

[14] Figure 2 shows observed and modeled Hg^0 and CO at Okinawa during spring 2004. The frequent simultaneous increases in CO and Hg^0 concentrations reflect the influence

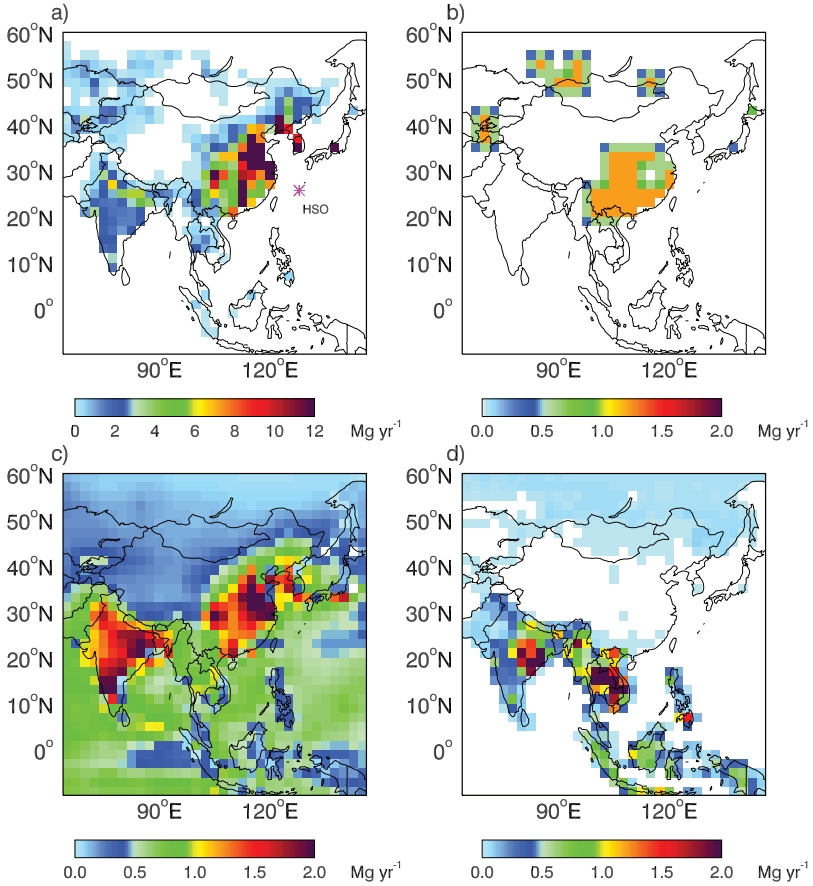

Figure 1. Distribution of annual Asian mercury emissions (Mg a^{-1}) from (a) anthropogenic, (b) geogenic, (c) land re-emission + ocean emission, and (d) biomass burning used in the GEOS-Chem model. The location of Okinawa is indicated by a star in Figure 1a.

of episodic outflow of polluted air from Asia reaching Okinawa [*Jaffe et al.*, 2005]. For CO, the mean observed value ± one standard deviation is 215 ± 65 ppbv compared to the modeled 209 ± 58 ppbv, while for Hg^0 the observed mean and standard deviation is 2.04 ± 0.38 ng m^{-3} standard air compared to the modeled 2.04 ± 0.25 ng m^{-3}. The model captures some of the observed temporal variability, with r^2 = 0.28 for CO and r^2 = 0.39 for Hg^0. The tagged simulations show that the variability in CO and Hg^0 is dominated by the variability in Asian tracers, as expected. For CO, the Asian anthropogenic tracer explains 97% of the variance in modeled total CO. Using multiple regression, we find that the Asian anthropogenic and land tracers together explain 97% of the variance in total Hg^0. Land emissions from Asia covary with the Asian anthropogenic tracer (r^2 = 0.87) due to the approximate colocation of the anthropogenic and land sources (Figure 1), which allows the tracers to be transported together.

[15] We used our tagged tracer simulation to divide the total CO and mercury concentrations over Okinawa into different source contributions for the 1 March to 31 May period (Table 1). Asian sources account for 44% of Hg^0 at Okinawa, with Asian anthropogenic, land, and biomass burning emissions contributing 26, 15, and 3%, respectively. The Asian anthropogenic contribution to Hg^{II} (45%) and particulate mercury (78%) over Okinawa is greater than the contribution to Hg^0 (Table 1) because the model shows Okinawa receiving direct transport of Asian Hg^{II} and particulate mercury emissions, but the short lifetimes of these species prevent them from reaching Okinawa by direct transport from other regions. For CO, the Asian anthropogenic contribution is 41%. During periods of enhanced outflow, the Asian anthropogenic contribution reaches up to 73% for CO and 43% for Hg^0 (Figure 2).

3.2. Hg^0 and CO at Mount Bachelor

[16] Figure 3 shows the time series of observed and modeled CO and TAM at MBO for 2004. At MBO, the mean model concentrations are 116 ± 20 ppbv and 1.61 ± 0.09 ng m^{-3} for CO and mercury, respectively, compared to observed means of 133 ± 28 ppbv and 1.53 ± 0.19 ng m^{-3}, yielding a mean model bias of −12% for CO and 5% for mercury. The CO bias is evident primarily in springtime. The r^2 value is 0.37 for CO and 0.34 for mercury. The model fails to reproduce the magnitude of the observed mercury peaks and has a standard deviation of only 0.09 ng m^{-3}. It also somewhat underestimates the standard deviation of CO. In contrast, the model better reproduces CO observations, including springtime long-range transport events, at the surface coastal site Cheeka Peak in Washington State [*Liang et al.*, 2004]. The difficulty at MBO is likely due to subgrid scale processes

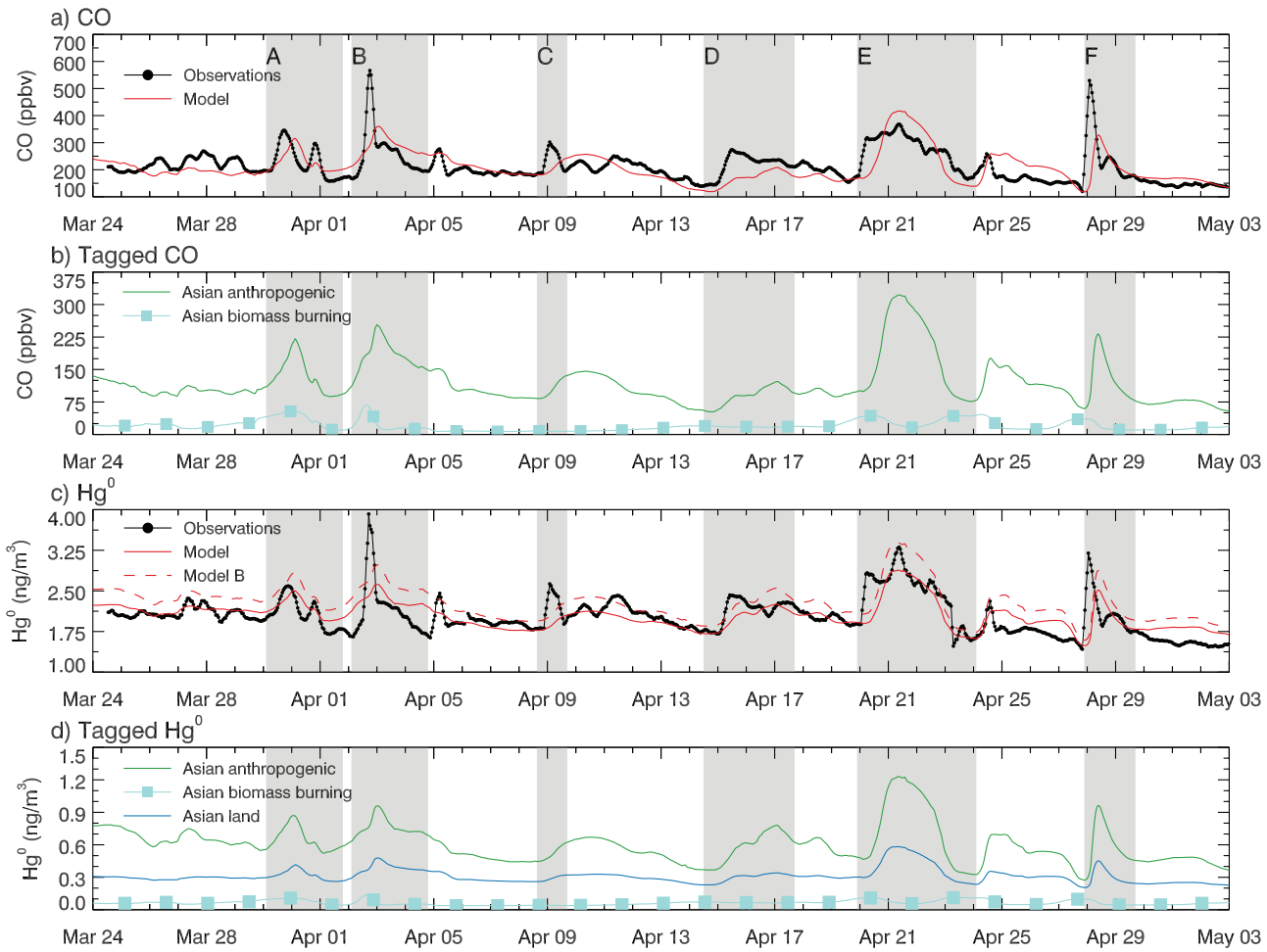

Figure 2. Time series of CO and Hg^0 at Okinawa for March–May 2004. (a) Observed (black) and modeled (red) CO. (b) Model CO tracers tagged by source. (c) Observed (black) and modeled (red) Hg^0. The dashed red line shows model simulation B (Asian Hg^0 emissions increased by 50%). (d) Hg^0 tracers tagged by source. The observations are averaged using a 6-h running mean. Asian transport events from *Jaffe et al.* [2005] are shaded in gray.

associated with the local mountainous terrain. The model grid box containing MBO has a surface altitude of 1.4 km above sea level. The model is sampled at the vertical level corresponding to the actual altitude of MBO (2.8 km above sea level), where the model captures the observed temperature. In the model, this level is usually above the boundary layer during spring. Springtime observations show that MBO experiences a mixture of boundary layer and free-tropospheric air, with a diurnal cycle in up-slope and downslope flow [*Weiss-Penzias et al.*, 2006]. Thus some of the model error is likely due to its inability to capture the transitions between boundary layer and free tropospheric air at the peak of Mount Bachelor.

[17] Unlike Okinawa, where enhancements are primarily driven by Asian transport, at MBO the tagged tracer simulations attribute the majority of the variability in CO to fluctuations in North American CO and CO from hydrocarbon oxidation, and much of the variability in mercury to variations in transport of regional land sources. During springtime, the North American land tracer explains 46% of the variability in TAM at MBO while the Asian tracers (anthropogenic + land + biomass burning) explain 42%. In the annual average, the North American land tracer explains only 29% of the TAM variability while the Asian tracers explain 57%. The large fraction of variability in the annual average explained by the Asian tracers is due partly to their effect on the seasonal cycle; the Asian tracers explain only 37% of the variance when monthly variability is removed by subtracting the 31-day running mean.

[18] *Weiss-Penzias et al.* [2007] discuss a number of Asian long-range transport events observed at MBO. The model captures some of these observed events (Figure 3). For the 9 and 10 April 2004 events (a, b), the model captures the timing of the events but greatly underestimates their magnitude. During the large 25 April event (c), the model shows a small enhancement in the Asian tracers for CO and mercury. However, the model predicts a larger Asian event 3 days later on 28 April. Our simulation captures the timing and duration of the 20 December event (h), and attributes it to concurrent increases in both the Asian and North American tracers. For several of the other observed events, there is a small increase in the Asian tracer corresponding to the timing of the event, but the model usually underestimates the magnitude of the events. This

Table 1. Average Springtime Contributions of Source Regions to Hg^0 (ng m^{-3}), Hg^{II} (pg m^{-3}), and CO (ppbv) at MBO, Okinawa, and the United States[a]

	Okinawa (26.8°N, 128.2°E, 60 m)			MBO (44.0°N, 121.7°W, 2.8 km)			USA (30°–46°N, 125°–65°W, Surf.)		
March 1–May 31	Hg^0	Hg^{II}	CO	Hg^0	Hg^{II}	CO	Hg^0	Hg^{II}	CO
Anthropogenic[b]									
Asia	0.48(26)	6.3(45)	73(41)	0.29(18)	15(18)	30(24)	0.26(16)	5.6(15)	25(16)
North America	0.03(2)	0.2(2)	11(6)	0.03(2)	2(2)	17(13)	0.07(4)	5.9(15)	53(31)
Europe	0.10(5)	0.5(4)	20(11)	0.10(6)	4.8(6)	19(15)	0.10(6)	1.9(5)	19(12)
Rest of world[c]	0.12(7)	0.7(5)	3(2)	0.12(7)	7.0(8)	4(3)	0.11(7)	2.7(7)	4(2)
Biomass Burning[b]									
Asia	0.06(3)	0.4(3)	19(12)	0.05(3)	2.5(3)	10(8)	0.04(3)	1.1(3)	8(5)
Rest of world[d]	0.09(5)	0.5(4)	5(3)	0.08(5)	5.1(6)	6(5)	0.08(5)	2(5)	8(5)
Land[b,e]									
Asia	0.27(15)	1.4(10)	-	0.21(13)	11.1(13)	-	0.20(12)	4.3(11)	-
North America	0.12(7)	0.7(5)	-	0.16(10)	6.7(8)	-	0.27(16)	3.4(9)	-
Rest of world[f]	0.34(18)	2.0(14)	-	0.34(21)	19(22)	-	0.33(20)	7.3(17)	-
Primary ocean[g]	0.22(12)	1.3(9)	-	0.21(13)	12.3(14)	-	0.21(13)	4.7(12)	-
CO: Oxidation of CH_4 and BVOC	-	-	42(26)	-	-	39(32)	-	-	44(28)
Total	1.8(100)	14(100)	173(100)	1.6(100)	86(100)	125(100)	1.7(100)	39(100)	171(100)

[a]Percent contributions are given in parentheses.
[b]Each tagged tracer includes ocean re-emission.
[c]Includes all anthropogenic emissions from regions other than Asia, North America, and Europe.
[d]Includes all biomass burning outside of Asia.
[e]Land tracer includes both geogenic emissions and re-emissions from land.
[f]Includes land emissions from all regions except Asia and North America.
[g]Oceanic mercury that originates below the mixed layer is considered primary ocean.

underestimate is likely due to model resolution and the inability to capture the high concentrations of a thin plume.

[19] The modeled lifetime of total gaseous mercury in the northern hemisphere spring, calculated as the TGM concentration divided by the loss to deposition, is approximately 9 months, so concentrations at both Okinawa and MBO are influenced by global sources. MBO, though more distant from Asia, nevertheless receives 34% of its Hg^0 from Asian sources during spring. On average, these Asian sources include 0.34 ng m^{-3} (20%) from the Asian background, 0.11 ng m^{-3} (7%) from ocean re-emission of Asian emissions, and 0.12 ng m^{-3} (7%) from direct transport from Asia. Non-Asian land and primary ocean emissions are also major contributors at MBO, accounting for 31% and 13%, respectively. The North American anthropogenic contribution is only 2%, reflecting MBO's location upwind from most North American sources. The Asian anthropogenic percent contribution to Hg^0 at MBO shows little variability between seasons, with an Asian anthropogenic contribution of 18% in spring and in the annual average. In the model, the largest Asian Hg^0 contribution occurred on 28 April, when the Asian sources accounted for 41% of Hg^0 (Figure 3 and event c). Since the model underestimates the magnitude of the events, this modeled Asian contribution is likely an underestimate. For CO, the percent contribution is 24% in spring compared to 20% in the annual average. The stronger seasonality in CO reflects its shorter lifetime (~2 months) compared to the 9-month lifetime of TGM.

[20] If we consider the entire continental United States, we find a springtime North American anthropogenic contribution to surface Hg^0 concentrations of 4%, a N. American land contribution of 16%, an Asian anthropogenic contribution of 16%, and an Asian land contribution of 12%. The remainder comes from anthropogenic and land emissions from other regions of the world, biomass burning, and ocean emissions (Table 1).

3.3. Hg^0/CO Ratios

[21] Mercury emissions inventories remain highly uncertain. For the global inventory, the uncertainty is estimated to be ±25% for fuel combustion sources, ±30% for industrial processes, and a factor of 2–5 for waste disposal [*Pacyna et al.*, 2006]. The uncertainty in anthropogenic emissions from China is ±44% [*Streets et al.*, 2005]. Uncertainties in natural mercury emissions, with estimates varying by a factor of 4 [*Gustin and Lindberg*, 2006], as well as re-emissions of previously deposited mercury further complicate these estimates. *Streets et al.* [2006] estimate the uncertainty in CO emissions from China to be ±68%. However, Asian CO emissions inventories have also been constrained by comparison to ground-based, aircraft, and satellite observations [e.g., *Heald et al.*, 2003, 2004; *Palmer et al.*, 2003].

[22] A common method for estimating emissions based on observed concentration data is to use the ratio of two observed compounds [*Hansen et al.*, 1989]. *Jaffe et al.* [2005] report an Hg^0/CO ratio at Okinawa of 0.0053 ng m^{-3} $ppbv^{-1}$ for the spring 2004 observations, as listed in Table 2. Ratios for individual Asian transport events range from 0.0036–0.0074 ng m^{-3} $ppbv^{-1}$, with a mean of 0.0056 ng m^{-3} $ppbv^{-1}$ during Asian transport episodes [*Jaffe et al.*, 2005]. This is similar to the TGM/CO ratio of 0.0074 ng m^{-3} $ppbv^{-1}$ found in a Shanghai plume during the ACE-Asia campaign by *Friedli et al.* [2004] and the TAM/CO ratio of 0.0046 ± 0.0013 ng m^{-3} $ppbv^{-1}$ (mean ± stddev) for Asian long-range transport events at MBO [*Weiss-Penzias et al.*, 2007]. In contrast, *Weiss-Penzias et al.* [2007] observed a TAM/CO enhancement ratio of

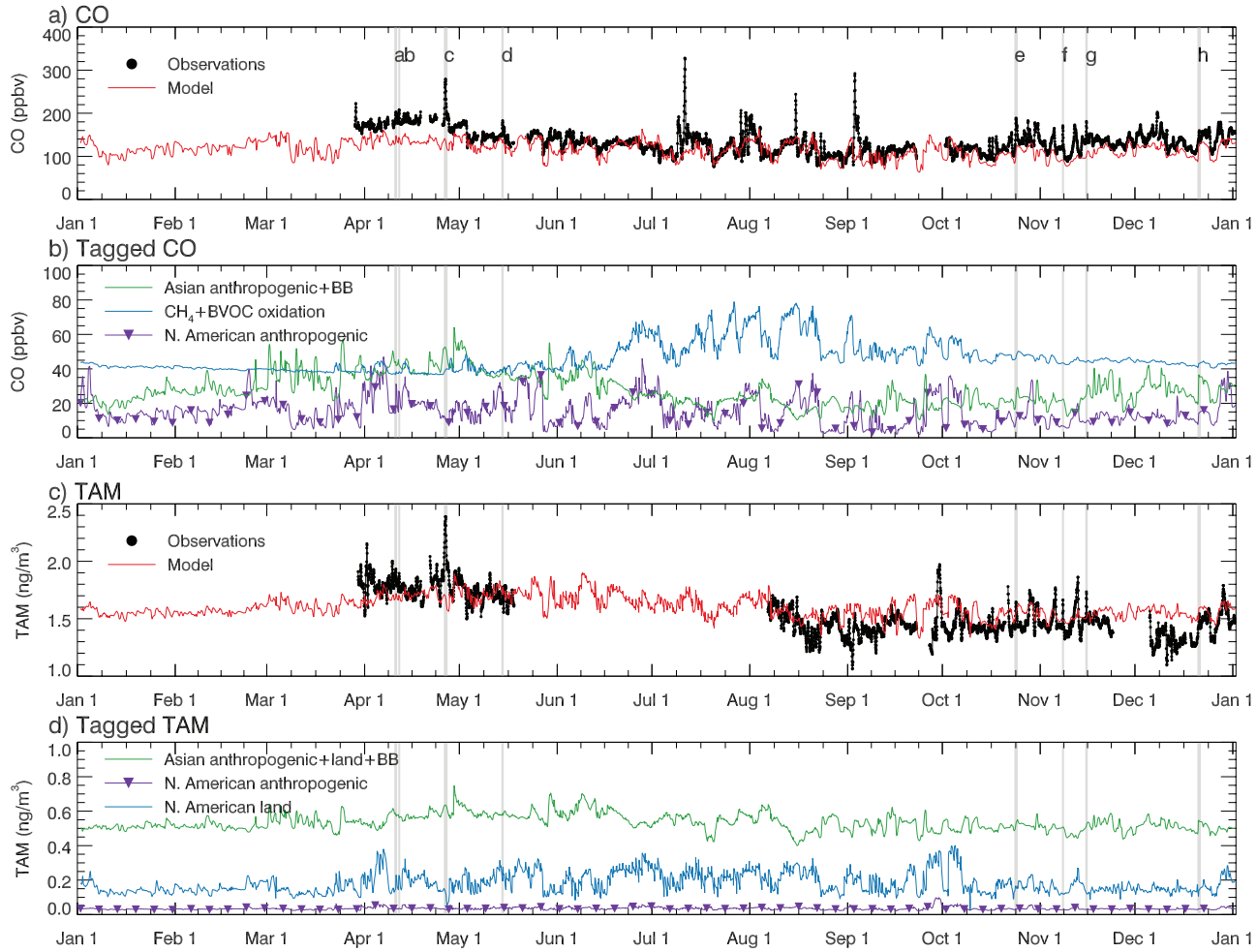

Figure 3. Time series of 6-h running mean observations and model at MBO for 2004. (a) Observed (black) and modeled (red) CO. (b) Model CO tracers tagged by source. (c) Observed (black) and modeled (red) total airborne mercury (TAM) from the standard simulation. (d) TAM tracers tagged by source. Asian long-range transport events from *Weiss-Penzias et al.* [2007] are shaded in gray and labeled Figures 3a–3h.

Table 2. Observed and Modeled Hg^0/CO Ratios (ng m^{-3} ppbv)

Location	Episode	Observations	Model	Model B[b]	Model C[c]	Model D[d]
Okinawa	spring 2004	0.0053	0.0039	0.0050	0.0062	0.0045
	A	0.0043	0.0044	0.0055	0.0066	0.0048
	B	0.0056	0.0029	0.0037	0.0045	0.0030
	C	0.0073	0.0045	0.0056	0.0068	0.0052
	D	0.0051	0.0065	0.0084	0.0103	0.0080
	E	0.0074	0.0044	0.0058	0.0072	0.0053
	F	0.0036	0.0050	0.0063	0.0076	0.0058
	HSO episode mean	0.0056	0.0046	0.0059	0.0072	0.0054
MBO	a	0.0032	0.0025	0.0024	0.0024	0.0026
	b	0.0035	0.0029	0.0029	0.0029	0.0032
	c	0.0042	0.0055	0.0057	0.0061	0.0063
	d	0.0048	0.0047	0.0044	0.0042	0.0045
	e	0.0026	0.0027	0.0033	0.0038	0.0030
	f	0.0044	0.0019	0.0032	0.0039	0.0030
	g	0.0051	0.0027	0.0033	0.0041	0.0029
	h	0.0051	0.0023	0.0034	0.0040	0.0031
	MBO 2004 Episode mean	0.0041	0.0031	0.0036	0.0039	0.0036
ACE-Asia[a]	04/30/01	0.0072	0.0061	0.0073	0.0087	0.0067

[a]The value is given for the Shanghai Plume in the ACE-Asia campaign [*Friedli et al.*, 2004].
[b]Model B has 280 Mg a^{-1} more Asian anthropogenic emissions and the same land emissions as the standard simulation.
[c]Model C has 610 Mg a^{-1} more Asian anthropogenic emissions and the same land emissions as the standard simulation.
[d]Model D repartitions the total emissions from the standard simulation with more anthropogenic emissions compensated by lower land emissions.

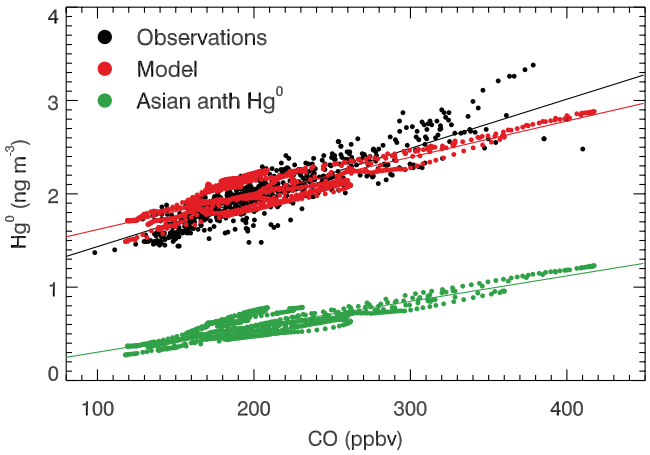

Figure 4. Scatterplot of Hg^0 (ng m^{-3}) versus CO (ppbv) concentrations for Okinawa 2004. Observations are in black, model in red, and model Asian tracer contribution in green. The mercury tracers are from the standard simulation.

0.0011 ng m^{-3} $ppbv^{-1}$ in U.S. industrial events and 0.0014 ng m^{-3} $ppbv^{-1}$ in biomass burning events.

[23] Using the observed ratio, *Jaffe et al.* [2005] calculated Asian Hg^0 emissions of 1460 Mg a^{-1} compared to 610 Mg a^{-1} Hg^0 in the anthropogenic inventory of *Pacyna et al.* [2006]. *Weiss-Penzias et al.* [2007] inferred Hg^0 emissions of 620 Mg a^{-1} from China, a factor of 2 larger than the recent anthropogenic inventory of 300 Mg a^{-1} from *Streets et al.* [2005] for China. The *Pacyna et al.* [2006] inventory for 2000 contains 360 Mg a^{-1} of Hg^0 emissions from China, 20% more than the *Streets et al.* [2005] inventory for 1999. *Pan et al.* [2006] compared a regional model with ACE-Asia data over the Yellow Sea and found that using Asian anthropogenic and biomass burning emissions of 1040 Mg a^{-1} total Hg with 830 Mg a^{-1} from Asian land, biogenic, and marine sources, their model underestimated mercury concentrations after subtracting background concentrations. They suggest that there may be an 80–200% underestimate in mercury emissions from China. Using 4D-Var to assimilate the ACE-Asia data, *Pan et al.* [2007] estimate Asian emissions of 1430–2270 Mg a^{-1} Hg^0, depending on their assumed boundary conditions.

[24] Here, we examine the ability of GEOS-Chem to reproduce observed Hg/CO ratios using the *Pacyna et al.* [2006] inventory. We sample the model hourly at Okinawa and find a slope of 0.0039 ng m^{-3} $ppbv^{-1}$, 26% lower than the observed slope of 0.0053 ng m^{-3} $ppbv^{-1}$ for the total data set (Table 2). Considering the ratios only during the Asian long-range transport events identified by *Jaffe et al.* [2005] yields a mean ratio of 0.0046 ng m^{-3} $ppbv^{-1}$, with a range of 0.0029–0.0065 ng m^{-3} $ppbv^{-1}$, 18% lower than the observed mean.

[25] In comparison to the previous studies described above, we find a smaller underestimate of Asian sources. The model's total Hg^0 tracer is able to capture the observed Hg^0/CO slope to within 30% because it includes a contribution from Asian land emissions and re-emissions. At Okinawa, these tracers covary in time with the Asian anthropogenic tracer and contribute to the magnitude of the observed events (Figure 2d). If we consider only the Asian anthropogenic tracer in the model, we get a slope of 0.0031 ng m^{-3} $ppbv^{-1}$, 42% lower than that observed (Figure 4). Anthropogenic emissions from other regions as well as Asian biomass burning also contribute to some of the events. However, since the model Hg^0/CO ratio is still lower than the observed ratio, we also examine the sensitivity of the model to higher Asian Hg^0 emissions.

[26] *Selin et al.* [2008] included a dry deposition sink for Hg^0 in the GEOS-Chem model and find that they need additional sources to balance this 1700 Mg a^{-1} loss. In particular, they increase the Asian anthropogenic Hg^0 source over the region 70°–152.5°E, 8°–45°N by 50% as well as increasing other anthropogenic sources and including artisanal mining. We conduct a simulation (Model B) by increasing the Asian anthropogenic source from 610 to 890 Mg a^{-1} Hg^0, but without including dry deposition of Hg^0 or increasing other sources. This simulation reproduces the observed Hg^0/CO slope for the total Okinawa data set (0.0050 ng m^{-3} $ppbv^{-1}$ modeled, 0.0053 ng m^{-3} $ppbv^{-1}$ observed) and the Asian transport events within 6%, but leads to a 13% positive bias in modeled Hg^0 for the total data set at Okinawa. Thus the Hg^0/CO ratio is consistent with a larger Asian anthropogenic source. However, lower background concentrations would be required to prevent model bias at Okinawa. Total Asian emissions of Hg^0 in this simulation are 1450 Mg a^{-1}. This estimate is smaller than the 2270 Mg a^{-1} of *Pan et al.* [2007] based on background concentrations of 1.2 ng m^{-3}, but agrees well with their estimate of 1430 Mg a^{-1} based on background concentrations of 1.5 ng m^{-3}. GEOS-Chem reproduces mean concentrations at nonurban land-based sites of 1.58 ng m^{-3} [*Selin et al.*, 2007]. Since the Hg^0/CO ratio at Okinawa is sensitive primarily to Hg^0 emissions, this improvement in the modeled ratio can be obtained either by increasing total emissions as described above, or by changing the speciation of the original emissions so that a larger fraction is emitted as Hg^0. *Edgerton et al.* [2006] found that 84% of the mercury in power plant plumes was Hg^0. Applying this speciation to the Asian emissions would lead to approximately a 50% increase in Asian Hg^0 (910 Mg a^{-1} Hg^0, 1470 Mg a^{-1} total Hg), leading to similar Asian Hg^0 emissions and a similar fit to observations compared with Model B.

[27] We conduct a third simulation (Model C) with Asian anthropogenic Hg^0 emissions over Asia doubled (1220 Mg a^{-1}) while other emissions are the same as in the base simulation. This yields a Hg^0/CO ratio of 0.0072 ng/m^3/ppbv for the Asian long-range transport events at Okinawa, a standard deviation above the observed mean (0.0056 ± 0.0016 ng m^{-3} $ppbv^{-1}$). For the total data set, we find a Hg^0/CO ratio of 0.0062 ng m^{-3} $ppbv^{-1}$ compared to the observed 0.0053 ng m^{-3} $ppbv^{-1}$. This simulation also leads to a 26% positive bias in Hg^0 concentrations at Okinawa, although this could potentially be reduced by inclusion of Hg^0 dry deposition. We therefore consider the doubling of Asian anthropogenic emissions an upper limit of the uncertainty.

[28] It is possible that an overestimate in the modeled land emissions could compensate for an underestimate in anthropogenic emissions. We examine this possibility with a model simulation (Model D) in which we decrease Asian

Table 3. Comparison of Asian and Chinese Hg^0 Emissions (Mg a^{-1}) From Several Studies[a]

Reference	Emissions: Asia	Emissions: China
Jaffe et al. [2005]	1460	
Pacyna et al. [2006]	(610)	(360)
Pan et al. [2007]	1430–2270	720–1140
Weiss-Penzias et al. [2007]		(620 ± 180)
Streets et al. [2005]		(300)
This study	1260–1450 (890–990)	680–800 (530–580)

[a]Values are given for emissions from all sources, while emissions from anthropogenic sources only are in parentheses.

Hg^0 land emissions and re-emissions by 70% (from 540 to 160 Mg a^{-1}) and increase Asian anthropogenic Hg^0 emissions by 62% (from 610 to 990 Mg a^{-1}) so that the total emissions are the same as the reference simulation. We do not alter the spatial distribution of the land or anthropogenic emissions. This simulation improves the agreement of the modeled and observed Hg^0/CO ratios for the total data set and agrees with the observed ratios during long-range transport events to within 2% (Table 2). It also increases the overall model Hg^0 bias at Okinawa from 2% to 7%.

[29] Mercury emitted from Asia as Hg^{II} and then reduced in the atmosphere can also contribute to the amount of Hg^0 reaching Okinawa during transport events. In-cloud reduction of Hg^{II} to Hg^0 in GEOS-Chem is scaled according to constraints on seasonal variability and TGM liftetime [*Selin et al.*, 2007]. Furthermore, *Edgerton et al.* [2006] suggest that in-plume reduction of RGM could explain their observations of RGM and Hg^0. To quantify the role of Hg^{II} emissions in our standard simulation, we conduct a model simulation without anthropogenic emissions of Hg^{II}. We find that removing direct Hg^{II} emissions decreases the model Hg^0/CO slope during Asian long-range transport events from 0.0046 ng m^{-3} $ppbv^{-1}$ to 0.0039 ng m^{-3} $ppbv^{-1}$ for Okinawa. This suggests that aqueous reduction of Hg^{II} emissions during transport contributes ~15% to the observed Hg^0/CO ratio at Okinawa.

[30] During the ACE-Asia campaign, *Friedli et al.* [2004] report a TGM/CO ratio of 6.4×10^{-6} w/w in a plume originating in Shanghai that they sampled on 30 April 2001. This is equivalent to 0.0072 ng m^{-3} $ppbv^{-1}$. We sample the model along the 30 April 2001 flight track and find a TGM/CO ratio of 0.0061 ng m^{-3} $ppbv^{-1}$, which would be 23% lower in the absence of Hg^{II} emissions. Increasing Asian emissions by 280 Mg a^{-1} (Simulation B) results in a TGM/CO ratio of 0.0073 ng m^{-3} $ppbv^{-1}$, in better agreement with the observed ratio (Table 2). *Friedli et al.* [2004] observed a peak in TGM concentrations between 6 and 7 km altitude, which they attribute to lofted pollution. Examining the vertical profile of Asian Hg^0 above Okinawa in the GEOS-Chem model, we also see episodic enhancements at this altitude.

[31] We also compare modeled and observed TAM/CO ratios at MBO during 8 Asian long-range transport events in 2004, as defined by *Weiss-Penzias et al.* [2007]. This leads to a modeled TAM/CO ratio of 0.0031 ng m^{-3} $ppbv^{-1}$ for the standard simulation, compared to the 2004 observed mean ratio of 0.0041 ng m^{-3} $ppbv^{-1}$ [*Weiss-Penzias et al.*, 2007]. Simulation B (50% increase in Asian anthropogenic Hg^0) yields an enhancement ratio of 0.0036 ng m^{-3} $ppbv^{-1}$ and an 11% positive model bias in Hg^0. Simulation C (doubled Asian anthropogenic Hg^0) results in a small underestimate of the enhancement ratio (0.0039 ng m^{-3} $ppbv^{-1}$) and a 20% positive model bias. Simulation D (62% higher Asian anthropogenic and 70% lower land emissions) similarly increases the modeled enhancement ratio to 0.0036 ng m^{-3} $ppbv^{-1}$ (Table 1) without changing the mean Hg^0 at MBO.

[32] We consider simulations B and D the best fit to the observations. This leads to an estimated range of Asian Hg^0 emission of 1260–1450 Mg a^{-1}, of which 890–990 is anthropogenic (Table 3). This represents approximately a 50% increase over the anthropogenic emissions estimate of *Pacyna et al.* [2006]. For China, we find Hg^0 emissions of 680–800 Mg a^{-1} of which 530–580 Mg a^{-1} is anthropogenic. This lies within the uncertainty given by *Weiss-Penzias et al.* [2007] and at the low end of the *Pan et al.* [2007] estimate, but our anthropogenic emissions are larger than the *Streets et al.* [2005] inventory (Table 3).

[33] We use GEOS-Chem at $4° \times 5°$ resolution to explore the effect of source regions on Hg^0/CO ratios globally. Figure 5 shows the Hg^0/CO regression slope for a 3-hourly time series in each model grid box at 930 hPa for April 2004. Slopes are only included where the Hg^0 versus CO regression yields $r^2 > 0.4$, and the standard deviation of CO exceeds 15% of mean CO. These criteria are met over and downwind of major source regions such as eastern China, Europe, and the eastern United States. In the southern hemisphere, South Africa and Australia are highlighted. We find large average Hg^0/CO ratios downwind of Asia (0.0040 ng m^{-3} $ppbv^{-1}$), and smaller ratios downwind of the eastern United States (0.0021 ng m^{-3} $ppbv^{-1}$) and Europe (0.0024 ng m^{-3} $ppbv^{-1}$). The highest Hg^0/CO ratio occurs near South Africa (0.0099 ng m^{-3} $ppbv^{-1}$), while outflow from Australia has a lower ratio of 0.0025 ng m^{-3} $ppbv^{-1}$. This supports the use of Hg^0/CO ratios as tracers of source regions. Care should be taken, however, in the interpretation of Hg/CO ratios as they reflect land as well as anthropogenic emissions of mercury. Furthermore,

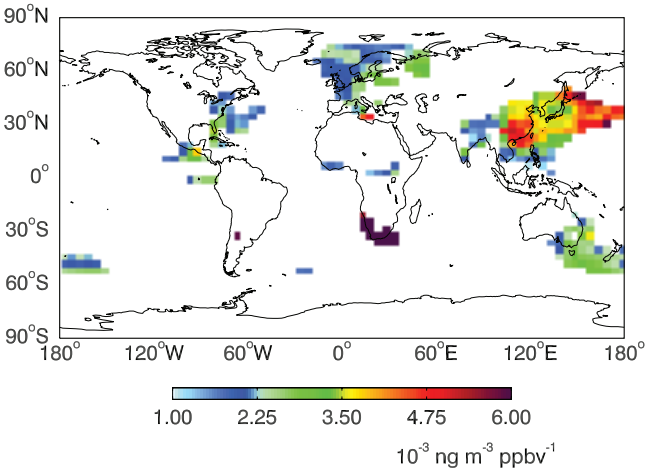

Figure 5. Hg^0/CO regression slopes for 3-hourly model output at 930 hPa for April 2004. Slopes are only given for grid boxes with a standard deviation of CO greater than 15% of mean CO and $r^2 > 0.4$ for the Hg^0/CO correlation.

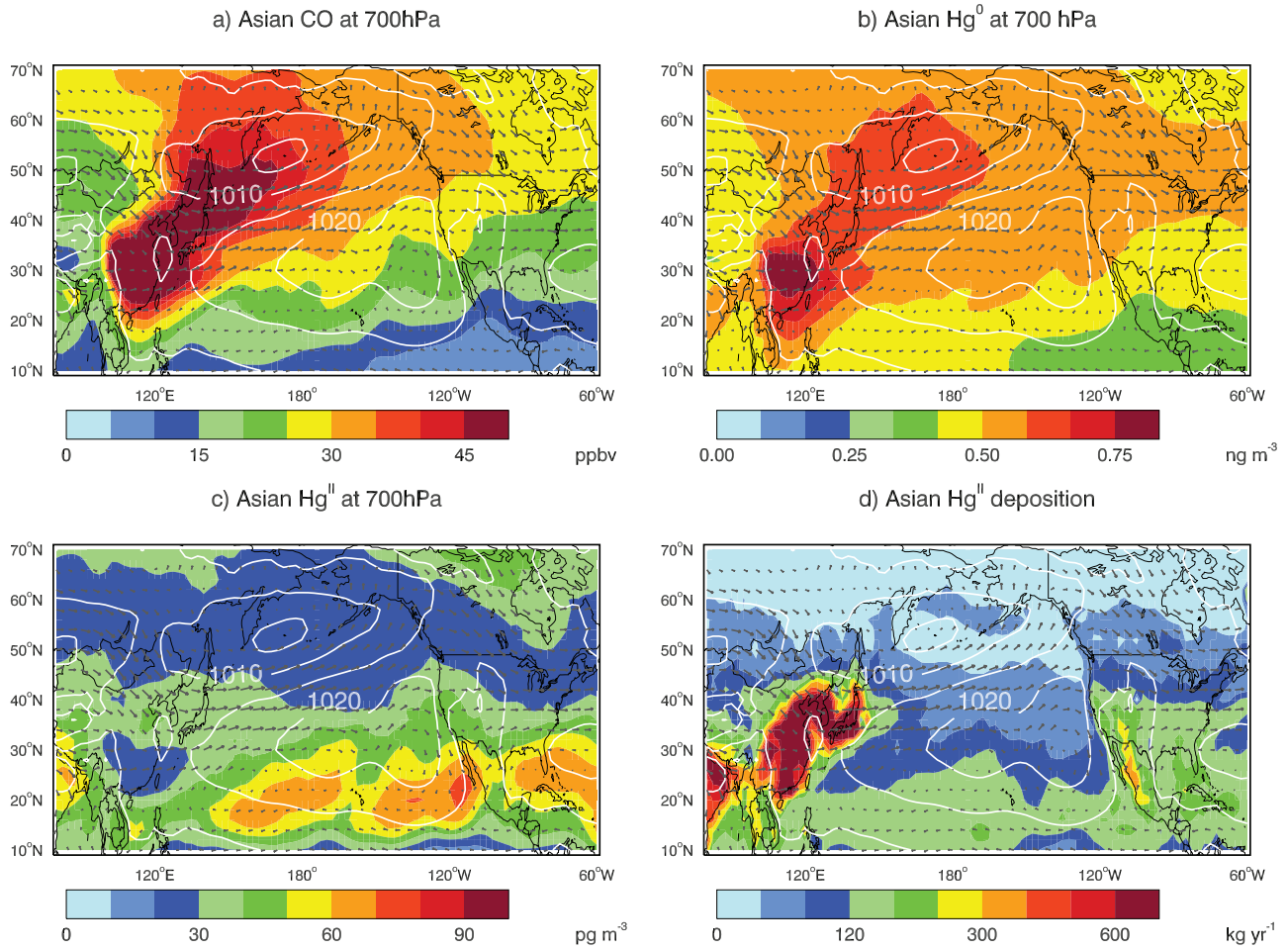

Figure 6. Map of March–May 2004 700 hPa concentrations of Asian (a) CO (ppbv), (b) Hg^0 (ng m^{-3}), and (c) Hg^{II} (pg m^{-3}) over the Pacific. Asian total deposition (kg a^{-1}) is shown in Figure 6d. Sea level pressure contours are overplotted in white, and gray arrows indicate wind at 700 hPa.

enhancement ratios may not be unique to a particular region. *Slemr et al.* [2006a] found TGM/CO ratios averaging 0.0050 ng m^{-3} $ppbv^{-1}$ at Mace Head, Ireland, similar to the ratios found in Asian outflow.

3.4. Trans-Pacific Transport of CO and Mercury

[34] The different mechanisms by which Asian Hg^0 and Hg^{II} reach North America affect the latitudinal distribution of their contributions (Figure 6). Hg^0, like CO, is transported to the northeast from Asia with the prevailing winds. Consequently, at 700 hPa the Asian influence is largest over Alaska, western Canada and the Northwestern United States (Figures 6a and 6b). In contrast, Asian emissions influence North American Hg^{II} concentrations through in situ oxidation of the global Asian Hg^0 pool rather than by direct advection of Hg^{II} from the emission source. The Asian Hg^{II} contribution is thus largest at low latitudes where high oxidant concentrations and descending dry air favor accumulation of Hg^{II} (Figure 6c). Total Hg^{II} concentrations are also high in this region for the same reason. Asian Hg^{II} deposition follows a similar pattern to Asian Hg^{II} concentration since both wet and dry deposition depend on Hg^{II} concentrations. Hg^{II} deposition is also larger over land, where dry deposition velocity is high (Figure 6d). In terms of percent contribution from Asian sources, the geographic distribution and the deposition of Hg^{II} are similar to that of Hg^0 and CO (Figure 7). This similarity occurs because Hg^{II} originates from oxidation of the Hg^0 pool and thus reflects regional percent contributions to that pool.

[35] Figure 8 shows a longitudinal cross-section of the contribution of CO, Hg^0, and Hg^{II} from Asian sources across the Pacific during spring. The contribution from Asian Hg^0 and CO decreases with distance from Asia, with Asian Hg^0 decreasing by 32% and CO decreasing by 56% at the surface between 140°E and 125°W. Both species show lower concentrations in the upper troposphere (Figures 8a and 8b). In contrast, Asian Hg^{II} increases at high altitudes, where it is not readily removed by wet or dry deposition or in-cloud reduction [*Selin et al.*, 2007]. Consequently, Asian Hg^{II} in the upper troposphere is due to oxidation of Asian Hg^0 emissions rather than to direct transport of Asian Hg^{II} emissions, which are mostly deposited close to their source (Figure 8c). The inverse altitude profiles of Hg^{II} and Hg^0 are consistent with observations at MBO [*Swartzendruber et al.*, 2006] and aircraft observations off the Florida coast [*Landis et al.*, 2005].

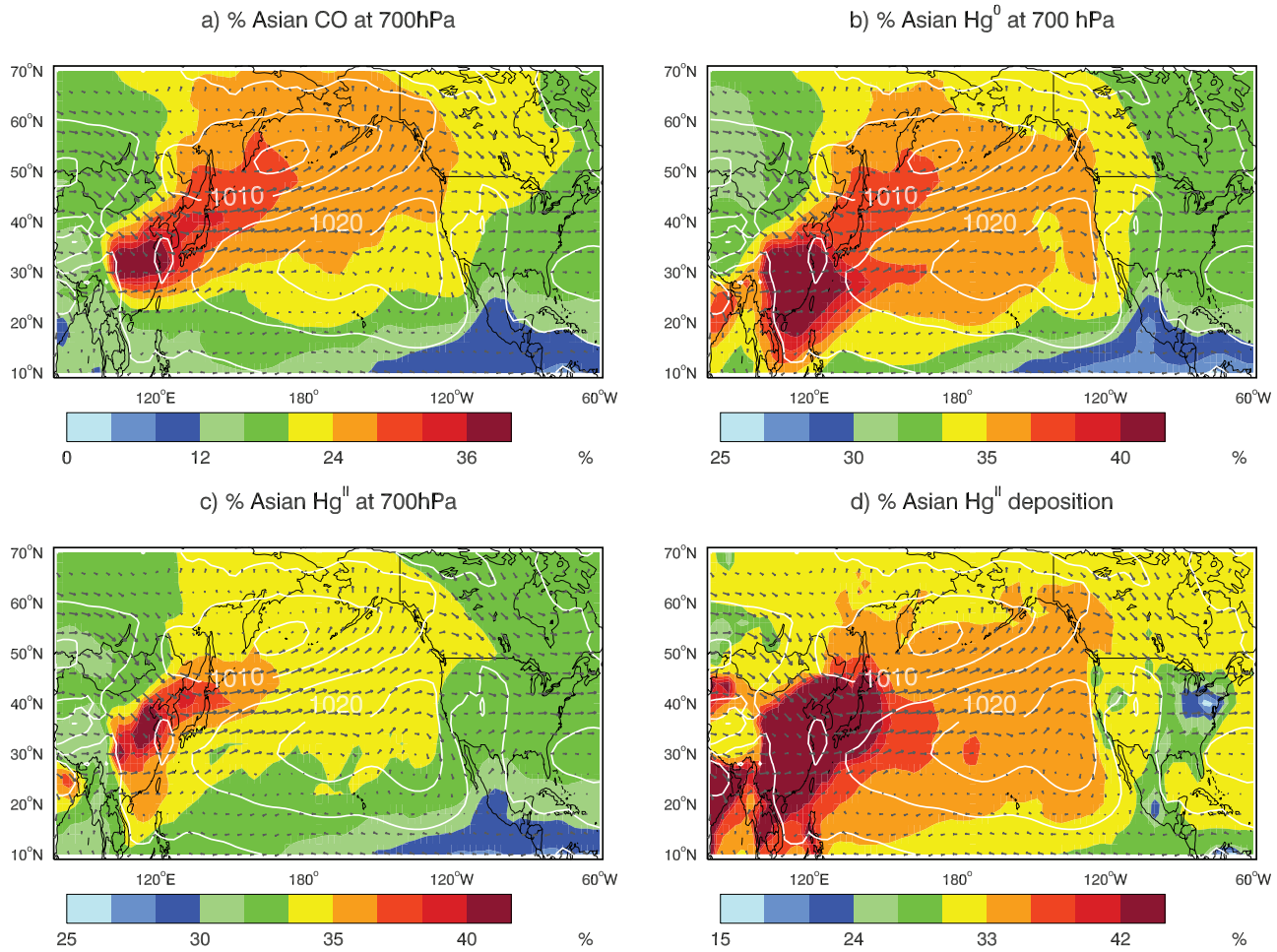

Figure 7. Map of March–May 2004 700 hPa percent contributions from the Asian tracers to (a) CO, (b) Hg^0, (c) Hg^{II}, and (d) total (wet + dry) deposition over the Pacific. Sea level pressure contours are overplotted in white, and gray arrows indicate wind direction.

[36] We consider the role Asian Hg^0 re-emitted from the ocean using a tagged simulation with ocean emissions turned off. We find that ocean re-emission increases the Asian contribution of Hg^0 over the west coast of North America by 29% (from 0.42 to 0.54 ng/m^3) (Figures 8b and 8d). Including Hg^0 ocean re-emissions increases the amount of Hg^0 available for oxidation and thus increases the background levels of Hg^{II} in the upper troposphere (Figures 8c and 8e).

3.5. Origin of Mercury Over the United States

[37] Table 4 shows regional contributions to Hg^{II} deposition (wet and dry) to Okinawa, MBO, and the United States. These contributions are based on the tagged tracer contributions in our standard simulation. Adding anthropogenic (including ocean re-emission) and land tracers together, we find a North American contribution to deposition over the continental United States of 26%, slightly lower than the 30% contribution of North American anthropogenic (direct + re-emission) to the US of *Seigneur et al.* [2004] and the 33% natural + anthropogenic North American contribution to deposition over North America of *Travnikov* [2005]. Our Asian land + anthropogenic deposition to the US is 25%, compared to 21% over the US [*Seigneur et al.*, 2004] and 24% over North America [*Travnikov*, 2005]. The Asian contribution in this study includes anthropogenic, geogenic, and land re-emission from Asia, as well as ocean re-emission of all those tracers. For comparison, *Seigneur et al.* [2004] include anthropogenic emissions from Asia and re-emission of those emissions from all regions, while *Travnikov* [2005] consider natural and anthropogenic emissions from Asia.

[38] The relative importance of Asian and North American sources to deposition over the U.S. varies geographically. We find that the average contribution to deposition in the western U.S. (125°–100°W) from the North American anthropogenic tracer is 11%, where as in the eastern U.S. (95°–75°W) the average contribution is 25% due to larger anthropogenic emissions in the eastern half of the country. This is similar to the results of *Selin et al.* [2007]. The Asian anthropogenic contribution to deposition is 15% over the western U.S. and 12% over the eastern U.S. For Hg^0 concentrations over the United States, the east-west gradient is smaller than for deposition, with approximately 15% coming from Asian anthropogenic sources in both the east and west of the country and the North American anthropogenic contribution increasing from 3% in the west to 6% in

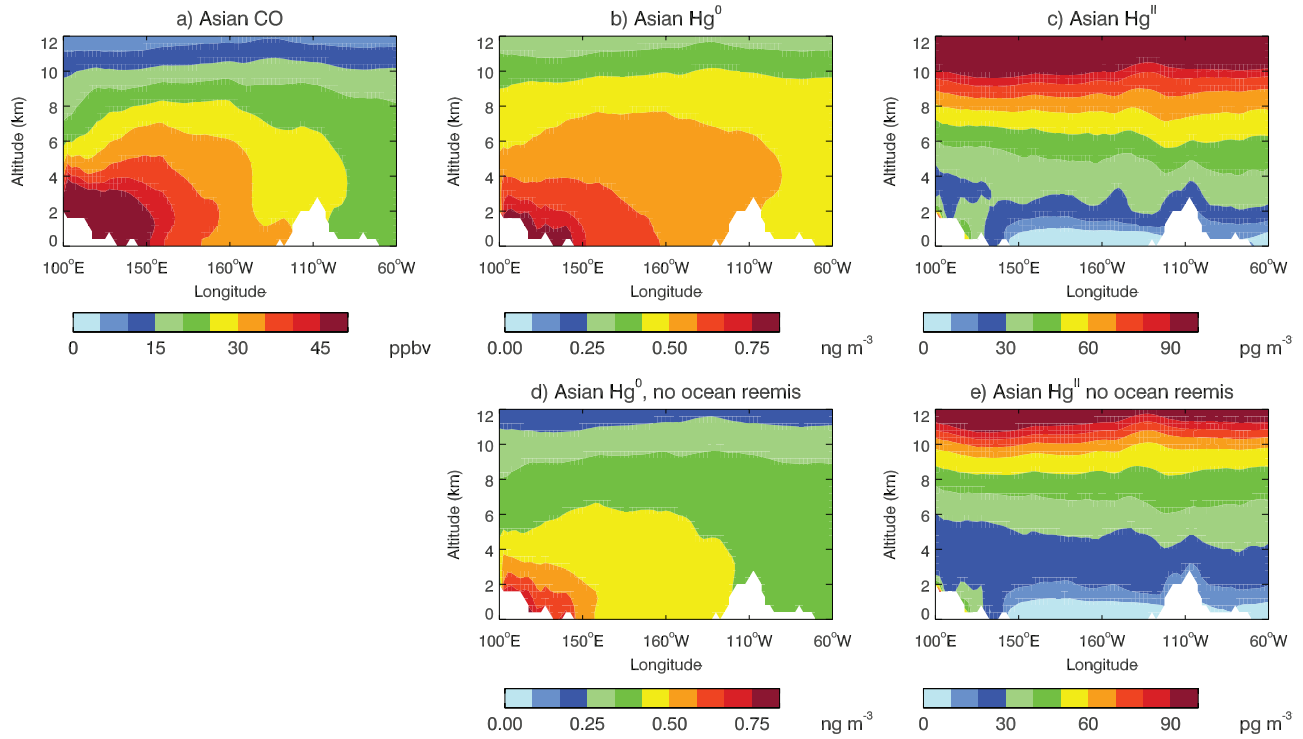

Figure 8. Longitude-altitude plot of Asian tracer concentrations averaged over 28°–60°N from 1 March to 31 May 2004 for (a) CO, (b) Hg^0 , and (c) Hg^{II}. Figures 8d and 8e show the Asian tracer concentrations excluding ocean re-emissions.

the east. The near-source deposition of Hg^{II} emissions drives the large east west gradient in deposition.

4. Conclusions

[39] We conducted a simulation of trans-Pacific transport of mercury including anthropogenic emissions tagged by region of origin as well as natural emissions and re-emissions from land and ocean. The simulation captures 39% of the observed variability in Hg^0 concentrations at Okinawa, Japan, and attributes the variability primarily to variability in the outflow of Asian anthropogenic and land emissions. At Mount Bachelor, Oregon, the model captures mean concentrations (1.53 ± 0.19 ng/m^3 observed, 1.61 ± 0.09 ng/m^3 modeled) of Hg^0, but underestimates the magnitude of the observed long-range transport events.

[40] We tested the model's ability to reproduce observed Hg/CO enhancement ratio during Asian long-range transport using the *Pacyna et al.* [2006] inventory for anthropogenic emissions. By including transport of Asian land emissions, which covary in time with transport of Asian anthropogenic emissions, the model reproduces the observed Hg/CO enhancement ratios to within approximately 30%. However, the ratio is underestimated, suggesting that Asian emissions in the inventory may also be underestimated. Increasing Asian anthropogenic Hg^0 emissions by 50% improves the ratio, but leads to a positive bias in the mean concentration. Altering the speciation of the emissions to increase Hg^0 yields a similar result. Increasing Asian anthropogenic Hg^0 emissions by 62% while reducing Asian land emissions so that total Asian emission is unchanged also improves the Hg/CO ratio. Doubling Asian anthropogenic emissions leads to a 29% overestimate of the Hg/CO ratio. We find that approximately 15% of the Hg/CO enhancement ratio at Okinawa is due to reduction of Hg^{II} emissions during transport. We cannot conclusively separate the effect of anthropogenic versus land emissions, but total Asian Hg^0 emissions of 1260–1470 Mg/a from anthropogenic, land, and biomass burning in the region 65°–146°W, 9°S–60°N are consistent with observations.

[41] Trans-Pacific transport of Hg^0 follows similar patterns to CO in both its latitudinal and vertical distribution. At MBO, we find a springtime Asian anthropogenic contribution to Hg^0 concentrations of 18% compared to a North American anthropogenic contribution of 2%. Including land emissions, these contributions increase to 31% and 12%, respectively. Ocean re-emission accounts for 22% of the Asian anthropogenic influence over the west coast of North America. Unlike Hg^0, Hg^{II} is not transported across the

Table 4. Annual Mean Percent Contribution to Wet and Dry Deposition of Hg^{II}

Annual Mean Deposition	%	Okinawa	MBO	USA
Anthropogenic	Asia	35	14	14
	N. America	1	19	16
	Europe	4	5	5
	rest of world	7	6	7
Biomass burning	Asia	2	2	2
	rest of world	5	5	5
Land	Asia	11	11	11
	N. America	6	9	10
	rest of world	17	17	18
Ocean	primary	12	12	12

Pacific in the lower troposphere due to its short lifetime, but the long lifetime of Hg^{II} in the upper troposphere allows global transport.

[42] **Acknowledgments.** This work was supported by funding from the National Science Foundation grant ATM 0238530.

References

Bey, I., D. J. Jacob, R. M. Yantosca, J. A. Logan, B. D. Field, A. M. Fiore, Q. Li, H. Y. Liu, L. J. Mickley, and M. G. Schultz (2001), Global modeling of tropospheric chemistry with assimilated meteorology: Model description and evaluation, *J. Geophys. Res.*, *106*, 23,073–23,095.

Duncan, B. N., R. V. Martin, A. C. Staudt, R. Yevich, and J. A. Logan (2003), Interannual and seasonal variability of biomass burning emissions constrained by satellite observations, *J. Geophys. Res.*, *108*(D2), 4100, doi:10.1029/2002JD002378.

Duncan, B. N., J. A. Logan, I. Bey, I. A. Megretskaia, R. M. Yantosca, P. C. Novelli, N. B. Jones, and C. P. Rinsland (2007), The global budget of CO, 1988–1997: Source estimates and validation with a global model, *J. Geophys. Res.*, *112*, D22301, doi:10.1029/2007JD008459.

Edgerton, E. S., B. E. Hartsell, and J. J. Jansen (2006), Mercury speciation in coal-fired power plant plumes observed at three surface sites in the southeastern U.S., *Environ. Sci. Technol.*, *40*, 4563–4570.

Friedli, H. R., L. F. Radke, and R. Prescott (2004), Mercury in the atmosphere around Japan, Korea, and China as observed during the 2001 ACE-Asia field campaign: Measurements, distributions, sources, and implications, *J. Geophys. Res.*, *109*, D19S25, doi:10.1029/2003JD004244.

Gustin, M. S., and S. E. Lindberg (2006), Terrestrial mercury fluxes: Is the net exchange up, down, or neither, in *Dynamics of Mercury Pollution on Regional and Global Scales: Atmospheric Processes and Human Exposures Around the World*, edited by N. Pirrone and K. R. Mahaffey, pp. 241–259, Springer, Norwell, Mass.

Hansen, A. D. A., T. J. Conway, L. P. Steele, B. A. Bodhaine, K. W. Thoning, P. Tans, and T. Novakov (1989), Correlations among combustion effluent species at Barrow, Alaska: Aerosol black carbon, carbon dioxide, and methane, *J. Atmos. Chem.*, *9*, 283–299.

Heald, C. L., et al. (2003), Asian outflow and trans-Pacific transport of carbon monoxide and ozone pollution: An integrated satellite, aircraft, and model perspective, *J. Geophys. Res.*, *108*(D24), 4804, doi:10.1029/2003JD003507.

Heald, C. L., D. J. Jacob, D. B. A. Jones, P. I. Palmer, J. A. Logan, D. G. Streets, G. W. Sachse, J. C. Gille, R. N. Hoffman, and T. Nehrkorn (2004), Comparative inverse analysis of satellite (MOPITT) and aircraft (TRACE-P) observations to estimate Asian sources of carbon monoxide, *J. Geophys. Res.*, *109*, D23306, doi:10.1029/2004JD005185.

Jaffe, D., E. Prestbo, P. Swartzendruber, P. Weiss-Penzias, S. Kato, A. Takami, S. Hatakeyama, and Y. Kajii (2005), Export of atmospheric mercury from Asia, *Atmos. Environ.*, *39*, 3029–3038.

Landis, M. S., M. M. Lynam, and R. K. Stevens (2005), The monitoring and modeling of mercury species in support of local, regional, and global modeling, in *Dynamics of Mercury Pollution on Regional and Global Scales*, edited by N. Pirrone and K. R. Mahaffy, Springer, New York.

Liang, Q., J. Jaeglé, D. A. Jaffe, P. Weiss-Penzias, A. Heckman, and J. A. Snow (2004), Long-range transport of Asian pollution to the northeast Pacific: Seasonal variations and transport pathways of carbon monoxide, *J. Geophys. Res.*, *109*, D23S07, doi:10.1029/2003JD004402.

Mason, R. P., and G.-R. Sheu (2002), Role of the ocean in the global mercury cycle, *Global Biogeochem. Cycles*, *16*(4), 1093, doi:10.1029/2001GB001440.

Pacyna, E., J. Pacyna, F. Steenhuisen, and S. Wilson (2006), Global anthropogenic mercury emission inventory for 2000, *Atmos. Environ.*, *40*, 4048–4063.

Palmer, P. I., D. J. Jacob, D. B. A. Jones, C. L. Heald, R. M. Yantosca, and J. A. Logan (2003), Inverting for emissions of carbon monoxide from Asia using aircraft observations over the western Pacific, *J. Geophys. Res.*, *108*(D21), 8828, doi:10.1029/2003JD003397.

Pan, L., J.-H. Woo, G. R. Carmichael, Y. Tang, H. R. Friedli, and L. F. Radke (2006), Regional distribution and emissions of mercury in east Asia: A modeling analysis of Asian Pacific Regional Aerosol Characterization Experiment (ACE-Asia) observations, *J. Geophys. Res.*, *111*, D07109, doi:10.1029/2005JD006381.

Pan, L., T. Chai, G. R. Carmichael, Y. Tang, D. Streets, J.-H. Woo, H. R. Friedli, and L. F. Radke (2007), Top-down estimate of mercury emissions in China using four-dimensional variational data assimilation, *Atmos. Environ.*, *41*, 2804–2819.

Seigneur, C., K. Vijayaraghavan, K. Lohman, P. Karamchandani, and C. Scott (2004), Global source attribution for mercury deposition in the United States, *Environ. Sci. Technol.*, *38*, 555–569.

Selin, N. E., D. J. Jacob, R. J. Park, R. M. Yantosca, S. Strode, L. Jaeglé, and D. Jaffe (2007), Chemical cycling and deposition of atmospheric mercury: Global constraints from observations, *J. Geophys. Res.*, *112*, D02308, doi:10.1029/2006JD007450.

Selin, N. E., D. J. Jacob, R. M. Yantosca, S. Strode, L. Jaeglé, and E. M. Sunderland (2008), Global 3-D land-ocean-atmosphere model for mercury: Present-day vs. preindustrial cycles and anthropogenic enrichment factors for deposition, *Global Biogeochem. Cycles*, *22*, GB2011, doi:10.1029/2007GB003040.

Slemr, F., R. Ebinghaus, P. G. Simmonds, and S. G. Jennings (2006a), European emissions of mercury derived from long-term observations at Mace Head, on the western Irish coast, *Atmos. Environ.*, *40*, 6966–6974.

Slemr, F., R. Ebinghaus, A. Zahn, and C. A. M. Brenninkmeijer (2006b), Distribution of gaseous mercury in the upper troposphere and lower dtratosphere as observed by CARIBIC flights, poster, EGU.

Streets, D. G., J. Hao, Y. Wu, J. Jiang, M. Chan, H. Tian, and X. Feng (2005), Anthropogenic mercury emissions in China, *Atmos. Environ.*, *39*, 7789–7806.

Streets, D. G., Q. Zhang, L. Wang, K. He, J. Hao, Y. Wu, Y. Tang, and G. R. Carmichael (2006), Revisiting China's CO emissions after the Transport and Chemical Evolution over the Pacific (TRACE-P) mission: Synthesis of inventories, atmospheric modeling, and observations, *J. Geophys. Res.*, *111*, D14306, doi:10.1029/2006JD007118.

Strode, S. A., L. Jaeglé, N. E. Selin, D. J. Jacob, R. J. Park, R. M. Yantosca, R. P. Mason, and F. Slemr (2007), Air-sea exchange in the global mercury cycle, *Global Biogeochem. Cycles*, *21*, GB1017, doi:10.1029/2006GB002766.

Swartzendruber, P. C., D. A. Jaffe, E. M. Prestbo, P. Weiss-Penzias, N. E. Selin, R. Park, D. J. Jacob, S. Strode, and L. Jaeglé (2006), Observations of reactive gaseous mercury in the free troposphere at the Mount Bachelor Observatory, *J. Geophys. Res.*, *111*, D24301, doi:10.1029/2006JD007415.

Talbot, R., et al. (2007), Factors influencing the large-scale distribution of Hg^0 in the Mexico City area and over the North Pacific, *Atmos. Chem. Phys. Discuss.*, *7*, 15,533–15,563.

Travnikov, O. (2005), Contribution of the intercontinental atmospheric transport to mercury pollution in the Northern Hemisphere, *Atmos. Environ.*, *39*, 7541–7548.

Weiss-Penzias, P., D. A. Jaffe, P. Swartzendruber, J. B. Dennison, D. Chand, W. Hafner, and E. Prestbo (2006), Observations of Asian air pollution in the free troposphere at Mount Bachelor Observatory during the spring of 2004, *J. Geophys. Res.*, *111*, D10304, doi:10.1029/2005JD006522.

Weiss-Penzias, P., D. Jaffe, P. Swartzendruber, W. Hafner, D. Chand, and E. Prestbo (2007), Quantifying Asian and biomass burning sources of mercury using the Hg/CO ratio in pollution plumes observed at the Mount Bachelor Observatory, *Atmos. Environ.*, *41*, 4366–4379.

Wilson, S., F. Steenhuisen, J. Pacyna, and E. Pacyna (2006), Mapping the spatial distribution of global anthropogenic mercury atmospheric emission inventories, *Atmos. Environ.*, *40*, 4621–4632.

C. Holmes, N. E. Selin, and R. M. Yantosca, School of Engineering and Applied Sciences and Department of Earth and Planetary Sciences, Harvard University, 29 Oxford St., Cambridge, MA 02138, USA.

L. Jaeglé, S. A. Strode, and P. C. Swartzendruber, Department of Atmospheric Sciences, University of Washington, 408 ATG Building, Box 351640, Seattle, WA 98195-1640, USA. (sstrode@atmos.washington.edu)

D. A. Jaffe, Interdisciplinary Arts and Sciences Department, University of Washington, Box 358530, Bothell, WA 98011, USA.